

Supplementary Material for: End-to-End Learned, Optically Coded Super-Resolution SPAD Camera

QILIN SUN, King Abudullah University of Science and Technology

JIAN ZHANG, Peking University

XIONG DUN, Tongji University

BERNARD GHANEM, King Abudullah University of Science and Technology

YIFAN PENG, Stanford University

WOLFGANG HEIDRICH, King Abudullah University of Science and Technology

1 FABRICATION DETAILS

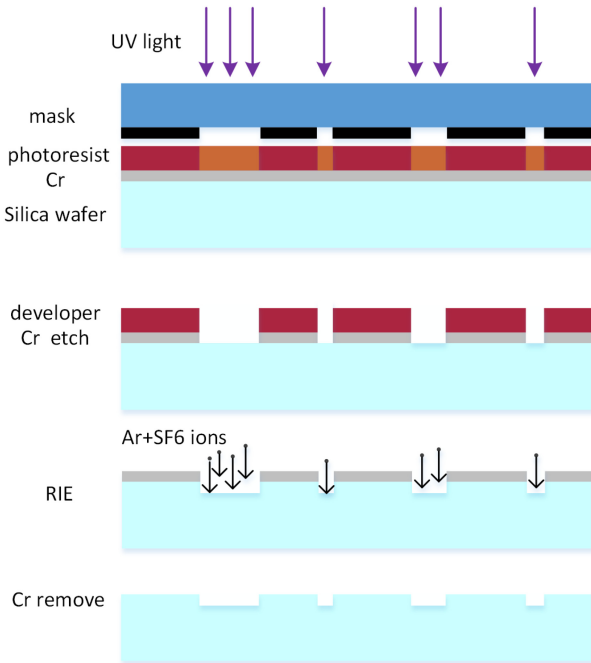


Fig. 1. Steps of DOE fabrication. First, patterns are transferred from masks to photoresist on the Fused Silica wafer through the exposure under UV illumination and the following develop process. Then, the transferred patterns are converted to binary profiles on the wafer by Cr etching and reactive ion beam ($\text{Ar} + \text{SF}_6$) bombardment. The final binary profile is obtained by removing the Cr layer.

As mentioned in the main text, the designed phase plates are discretized to eight height levels, which can then be realized by repeatedly applying the photolithography and reactive ion etch (RIE) process three times [2]. The core of fabrication (i.e., photolithography and RIE) is shown in Figure 1. The thickness of the Cr layer

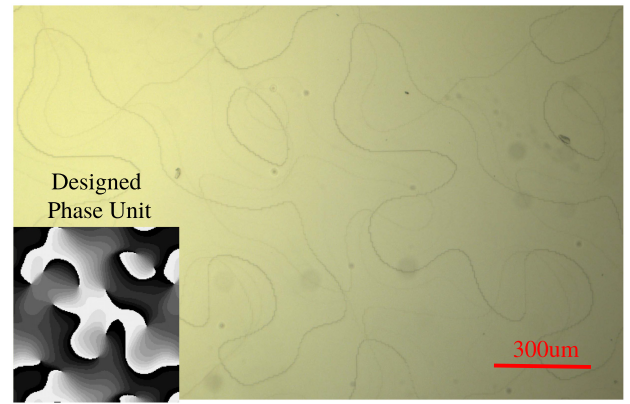


Fig. 2. 5X microscope images of a fabricated DOE.

is 100 nm, and the etching depths for each circle are 178, 356, and 712 nm sequentially.

The microscope images of fabricated diffractive phase plates are shown in Figure 2. Each phase unit is designed as 0.873×0.873 mm, and we repeat 16×16 units for the final diffractive phase plate. With this kind of repeatable designing scheme, our phase plates fit well with different sizes of aperture, exhibiting an aperture-invariant PSF behaviour. In addition, our designed phase unit has a smooth and continuous profile. This releases the requirement of a very high precision fabrication method. For commercial use, one can use state-of-the-art micro-stamp methods [3] to fabricate the phase plates in a low budget.

2 ADDITIONAL RESULTS

Simulations. We present selected visualization results tested on well-known image datasets, as shown in Figure 3 and Figure 4. For insets of each group, GT represents the ground truth image. The four different sampling models include (1) the *low fill-factor* model, which uses the SPAD sensor model but without the phase plate; (2) the *full fill-factor* model, which uses the full fill-factor

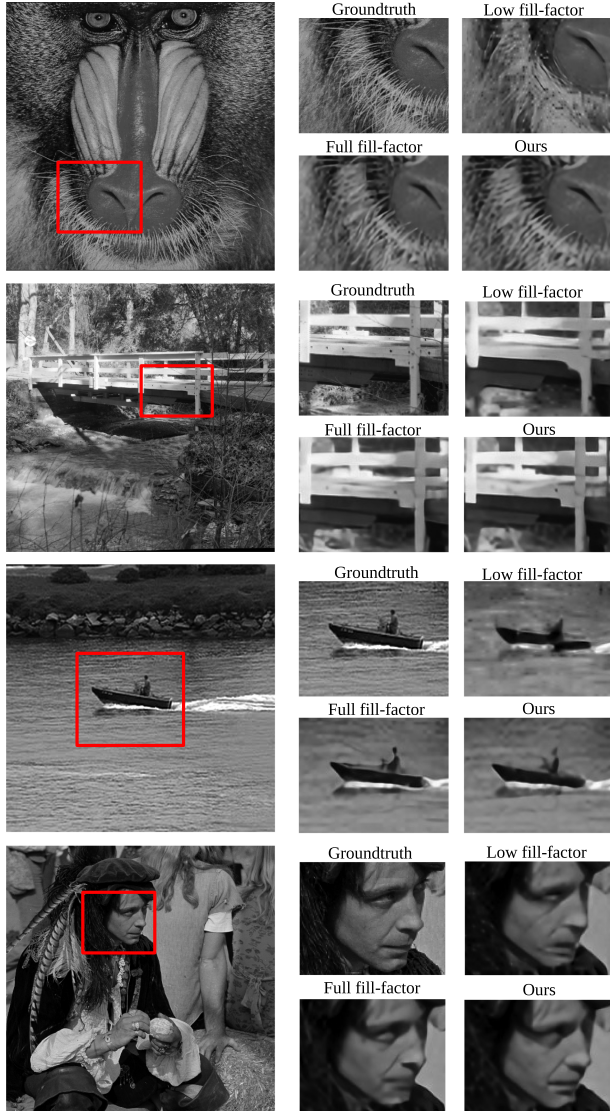


Fig. 3. Selected examples from Set14 [4] for the comparison of a 4 \times super-resolution effect with different sampling models.

sensor model without a phase plate as an additional comparison, as it is a very common sensor model; and (3) *our* model, which uses the SPAD sensor model with the phase plate optimized using our end-to-end framework.

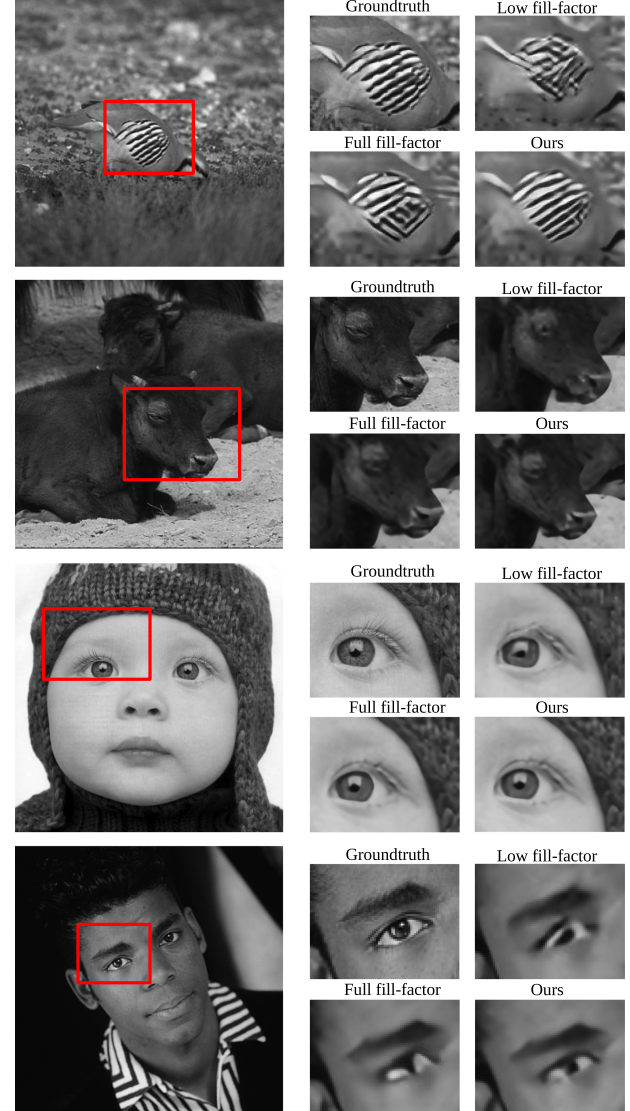


Fig. 4. Selected examples from BSDS100 [1] for the comparison of a 4 \times super-resolution effect with different sampling models.

REFERENCES

- [1] Pablo Arbelaez, Michael Maire, Charless Fowlkes, and Jitendra Malik. 2011. Contour detection and hierarchical image segmentation. *IEEE Transactions on Pattern Analysis and Machine Intelligence* 33, 5 (2011), 898–916.
- [2] Brian Morgan, Christopher M. Waits, John Krizmanic, and Reza Ghodssi. 2004. Development of a deep silicon phase Fresnel lens using gray-scale lithography and deep reactive ion etching. *Journal of Microelectromechanical Systems* 13, 1 (2004), 113–120.
- [3] Dong Qin, Younan Xia, and George M. Whitesides. 2010. Soft lithography for micro-and nanoscale patterning. *Nature Protocols* 5, 3 (2010), 491.
- [4] Roman Zeyde, Michael Elad, and Matan Protter. 2010. On single image scale-up using sparse-representations. In *Proceedings of the International Conference on Curves and Surfaces*. 711–730.